Single-Layered Imine-Linked Porphyrin-Based Two-Dimensional Covalent Organic Frameworks Targeting CO₂ Reduction

Nicolás Arisnabarreta,* Yansong Hao, Enquan Jin, Aude Salamé, Klaus Muellen, Marc Robert,* Roberto Lazzaroni, Sandra Van Aert, Kunal S. Mali,* and Steven De Feyter*

The reduction of carbon dioxide (CO_2) using porphyrin-containing 2D covalent organic frameworks (2D-COFs) catalysts is widely explored nowadays. While these framework materials are normally fabricated as powders followed by their uncontrolled surface heterogenization or directly grown as thin films (thickness >200 nm), very little is known about the performance of substrate-supported single-layered (≈0.5 nm thickness) 2D-COFs films (s2D-COFs) due to its highly challenging synthesis and characterization protocols. In this work, a fast and straightforward fabrication method of porphyrin-containing s2D-COFs is demonstrated, which allows their extensive high-resolution visualization via scanning tunneling microscopy (STM) in liquid conditions with the support of STM simulations. The as-prepared single-layered film is then employed as a cathode for the electrochemical reduction of CO_2. Fe porphyrin-containing s2D-COF@graphite used as a single-layered heterogeneous catalyst provided moderate-to-high carbon monoxide selectivity (82%) and partial CO current density (5.1 mA cm^{-2}). This work establishes the value of using single-layered films as heterogeneous catalysts and demonstrates the possibility of achieving high performance in CO_2 reduction even with extremely low catalyst loadings.

1. Introduction

The efficient conversion of CO_2 into value-added chemicals or fuels contributes to the carbon cycle and solving environmental problems. The electrochemical and photochemical carbon dioxide reduction reaction (CO_2RR) are well-studied nowadays.[1] Catalysts range from solid-state bulk metals to well-defined molecular catalysts, which can be easily tuned on demand. Particularly, metallated porphyrins and phthalocyanines belong to the most popular molecular catalysts and thus have been studied in various environments including homogeneous and heterogeneous conditions.[2,3]

Metal complexes of porphyrins and phthalocyanines can be incorporated into 2D covalent organic frameworks (2D-COFs)[4] that are actively tested as catalysts for electrochemical CO_2RR.[5,6] Such

N. Arisnabarreta, K. S. Mali, S. De Feyter
Division of Molecular Imaging and Photonics
Department of Chemistry
KU Leuven
Leuven B-3001, Belgium
E-mail: nicolas.arisnabarreta@kuleuven.be; kunal.mali@kuleuven.be; steven.defeyter@kuleuven.be
Y. Hao, S. Van Aert
Electron Microscopy for Materials Science (EMAT) and NANOlab Center of Excellence
University of Antwerp
Gronenborgerlaan 171, Antwerp 2610, Belgium

Y. Hao, R. Lazzaroni
Laboratory for Chemistry of Novel Materials
Materials Research Institute
University of Mons
Place du Parc 20, Mons 7000, Belgium
E. Jin, K. Muellen
Max Planck Institute for Polymer Research
Ackermannweg 10, 55128 Mainz, Germany
E. Jin
State Key Laboratory of Inorganic Synthesis and Preparative Chemistry
College of Chemistry and International Center of Future Science
Jilin University
Changchun 130012, P. R. China
A. Salamé, M. Robert
Université Paris Cité
Laboratoire d'Electrochimie Moléculaire
CNRS
Paris F-75006, France
E-mail: robert@u-paris.fr
M. Robert
Institut Universitaire de France (IUF)
Paris F-75005, France

ADVANCED
SCIENCE NEWS
www.advancedsciencenews.com

ADVANCED
ENERGY
MATERIALS
www.advenergymat.de

2D-COFs may be either fabricated as a bulk powder and immobilized at a given conductive surface or grown directly on the electrode as a thin film.[7–9] For example, Chang and coworkers [8] have compared the influence of the bulk 2D-COF surface immobilization process and its active site availability, which were found to be key factors for the resulting catalytic activity. They have reported high faradaic efficiencies (86%) of CO_2-to-CO conversion when employing a ~350 nm thick Co-porphyrin 2D-COF film on glassy carbon. Also, such 2D-COF film showed 7 times higher turn-over frequencies in comparison to the case where the same bulk 2D-COF is deposited on carbon fabric. Moreover, using Fe-porphyrin 2D-COF thin films fabricated on carbon cloths, Kubiak and coworkers have converted CO_2 to CO with efficiencies ≈80% and current densities of 0.5 mA cm^{-2}.[9]

Reducing the film thickness to few-layered or even single-layered films is attractive[6] due to (i) availability of the majority of the active sites within the framework; (ii) higher gas diffusion; and (iii) better charge transport through the material. Single-layered covalent organic frameworks (s2D-COFs) on electrodes may therefore offer a promising alternative to the use of thicker films or even 2D-COF powders. An additional advantage monolayer films bring is the possibility of direct molecular-level and structural characterization with high spatial resolution techniques such as scanning tunneling microscopy (STM) before, after, and even during the desired targeted catalysis, such as CO_2RR[10] and oxygen evolution.[11,12] The local probing of this technique offers the attractive prospect of identifying structural features, including defects, with (sub)monomer resolution and following in some cases even the dynamics of nucleation and growth.[13]

However, producing monolayer s2D-COF films on electrodes comes with a number of challenges. For the on-surface fabrication of single-layered imine-linked polymers,[14–26] a popular class of COFs, two main approaches can be distinguished. Upon synthesis at the solid/air interface,[17,18] variations in the conditions (i.e., deposition procedure, reaction temperature, and time) as well as ambient pressure and humidity are known to affect the success and quality of the s2D-COF. This protocol requires elevated temperature conditions. Conversely, the second method for imine-linked s2D-COF formation, namely the synthesis at the solid/liquid interface is simpler and proceeds well at room temperature or with mild heating only.[14–16] However, this approach proves effective only with a limited range of monomers and suffers from solubility issues for larger monomers such as porphyrins.

As reliable s2D-COF formation is a requisite for the use of the functionalized electrodes as catalysts for the electrochemical CO_2RR, we have initially focused on developing a procedure for the successful, fast, and reproducible fabrication of single-layered substrate-supported porphyrin-based imine-linked 2D-COFs films. Such single-layered frameworks on graphite were characterized via high-resolution STM imaging and their simulation counterparts. CO_2RR catalysis experiments using these novel single-layered Fe porphyrin showed higher efficiencies for the CO_2 to CO conversion in comparison to reported works using much thicker Fe-containing 2D-COF films. These results suggest that thicker films, i.e., higher catalyst loading, may not present better performances than thinner or even single-layered films of well-defined catalytic frameworks.
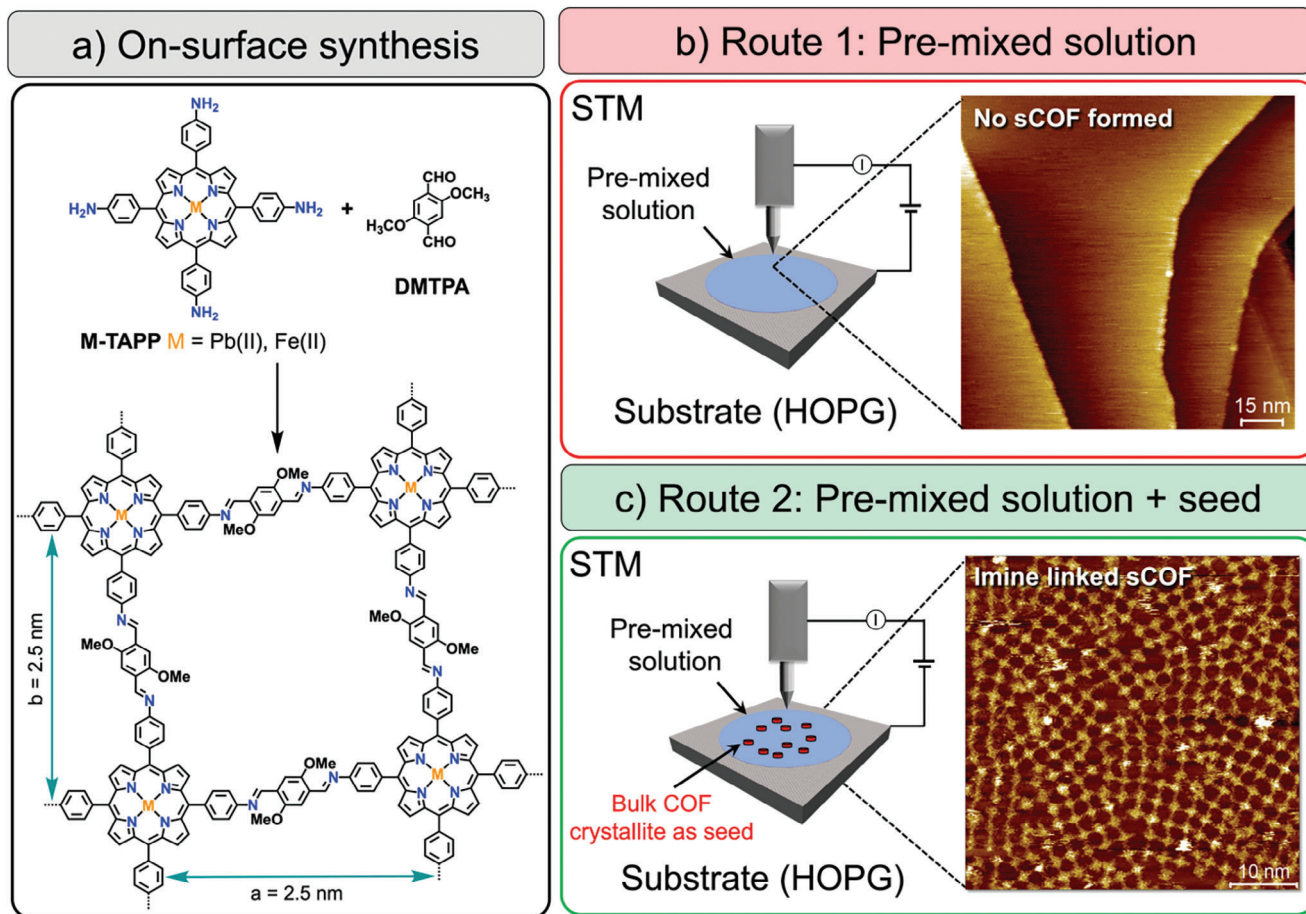
2. Results and Discussion

2.1. Designing Single-Layered Porphyrin-based 2D-COF Catalysts for CO_2RR

Aiming toward the conversion of CO_2 into value-added chemicals, we sought to design a substrate-supported single-layered 2D-COF heterogeneous catalyst bearing well-defined active sites and to develop a protocol for their reliable formation. Free-base and metal (M = Pb(II) and Fe(II)) containing tetra(4-aminophenyl)porphyrins (M-TAPP), and 2,5-dimethoxyterephthalaldehyde (DMTPA) were chosen as building blocks (see monomer synthesis in Section S1 in Supporting Information) for the fabrication of imine-linked s2D-COFs at the solid/liquid interface. Fe-containing porphyrins are relevant as catalysts since they exhibit high efficiencies for the electrochemical conversion of CO_2 into CO, both under homogeneous and heterogeneous conditions.[27,28] While Pb-porphyrins are not catalytically active for CO_2RR, they are well-suited for proving the s2D-COF formation at the solution-solid interface as well as nanoscale structural analysis using STM.[29] The chosen substrate was highly oriented pyrolytic graphite (HOPG) since it allows both the fabrication and high-resolution STM characterization of the single-layered framework[18] in ambient conditions as well as its usage as electrode for the CO_2RR.[30]

First, we targeted the synthesis of the s2D-COFs at room temperature at the HOPG/heptanoic acid (HA) interface. As shown in **Scheme 1**, the on-surface deposition of a pre-mixed solution (route 1) of both monomers, i.e., M-TAPP and DMTPA, did not give rise to the desired s2D-COF at the surface, regardless of the solution composition and the annealing conditions (Figure S1, Supporting Information). Note that the M-TAPP monomer itself also does not organize into a self-assembled molecular network (SAMN) at the solid/liquid interface.

Interestingly, the desired M-TAPP-based s2D-COF can only be fabricated at room temperature at the HOPG/HA interface, with high reproducibility (>85%), via the incorporation of a seed as shown in route 2 of Scheme 1. In this protocol, 5 µL of a pre-mixed solution of M-TAPP and DMTPA (30 and 45 µM, respectively) is drop casted on the HOPG surface followed by the deposition of a tiny amount (< 0.1 mg) of a free-base bulk-COF seed on the HOPG surface, covered by the previously drop casted solution (see Supporting Information for seed details). A metal-free seed is synthetically easily accessible and may be used independently of the targeted metal-containing s2D-COF. Various experiments support the hypothesis that the seed is depositing material, i.e., (partially) polymerized metal-free s2D-COF at the interface (see Figures S2 and S3, Supporting Information). In this scenario, the metal-containing s2D-COFs are fabricated by the reaction between the metal porphyrin monomers (M-TAPPs) and/or DMTPA with some patches from the seed for further on-surface polymerization (for more details, see Figure S3 in Supporting Information). The reasoning for using a seed was inspired by similar seed-based approaches which have been proven effective for the fabrication of boroxine-based s2D-COFs.[31] Additionally, a related seeding method was found to increase the surface coverage and reproducibility in the case of a 2-in-1 monomer imine-linked s2D-COF as well.[24] The seeding approach allows the straightforward fabrication of thin films of s2D-COFs on solid surfaces.

**ADVANCED
SCIENCE NEWS**

www.advancedsciencenews.com

**ADVANCED
ENERGY
MATERIALS**

www.advenergymat.de

Scheme 1. a) Reaction scheme showing the on-surface synthesis of metal atoms containing s2D-COFs. b) Route 1: Drop casting a pre-mixed solution results in an empty HOPG surface; and c) Route 2: Incorporation of a COF seed on top of the drop cast pre-mixture solution results in the successful, room temperature fabrication of s2D-COF, as revealed by STM.

It alleviates the typical challenges associated with the on-surface synthesis of s2D-COFs where the difference between adsorption enthalpies of the two monomers needs to be considered for initiating the 2D polymerization process while avoiding kinetic barriers. The latter may prohibit the dynamic polymerization process due to the preferential adsorption of one monomer. We believe that the added crystal acts as a seed whereby the reactive edges of the deposited material facilitate the nucleation of s2D-COF film on the surface. Furthermore, as we have demonstrated below, this approach also allows us to fabricate different metal-containing s2D-COF films while using the same free-base porphyrin 2D COF seed thus greatly simplifying the on-surface synthesis process.

Figure 1a shows a typical large-scale STM image of the Fe-s2D-COF obtained at the solid/liquid interface via the seeding method. It consists of patches of square lattices only, each only a few tens to hundreds of square nanometers in size, fully covering the surface (Figure S4, Supporting Information). The square lattice exhibits cross-like features, assigned to the porphyrins, which are linked together by a covalent bond via the reaction with the DMTPA linker leading to an imine bond. Not all squares show the same STM contrast. At this juncture, we attribute the distinct high-contrast cross-like features to the presence of Fe-containing porphyrins. Conversely, the less prominent, low-contrast features are generated by free-base porphyrins originated from the COF seed. The estimated free-base porphyrin content within the Fe-based framework is at a maximum of 15%, based on the analysis of the STM contrast in high-resolution STM images. The unit cell parameters ($a = b = 2.5 \pm 0.1$ nm, $\alpha = 90 \pm 1°$), obtained from calibrated STM images, are independent of the porphyrin monomer (see Table S1, Supporting Information). These parameters are in good agreement with molecular models,[14,17,32,33] and thus support the formation of s2D-COF (see also Figure S5, Supporting Information). High-resolution STM imaging reveals various types of structural defects found in the C4-symmetric frameworks such as regular pentagons as well as auto host-guest systems (Figure 1b,c). Different types of defects as well as surface dynamics (restructuring and s2D-COF expansion) were also imaged in the Pb-s2D-COF (Figure S6, Supporting Information).

2.2. Metal Presence in Single-Layered 2D-COF Catalyst

To substantiate the relationship between variations in STM contrast and the composition of the s2D-COFs, STM images are
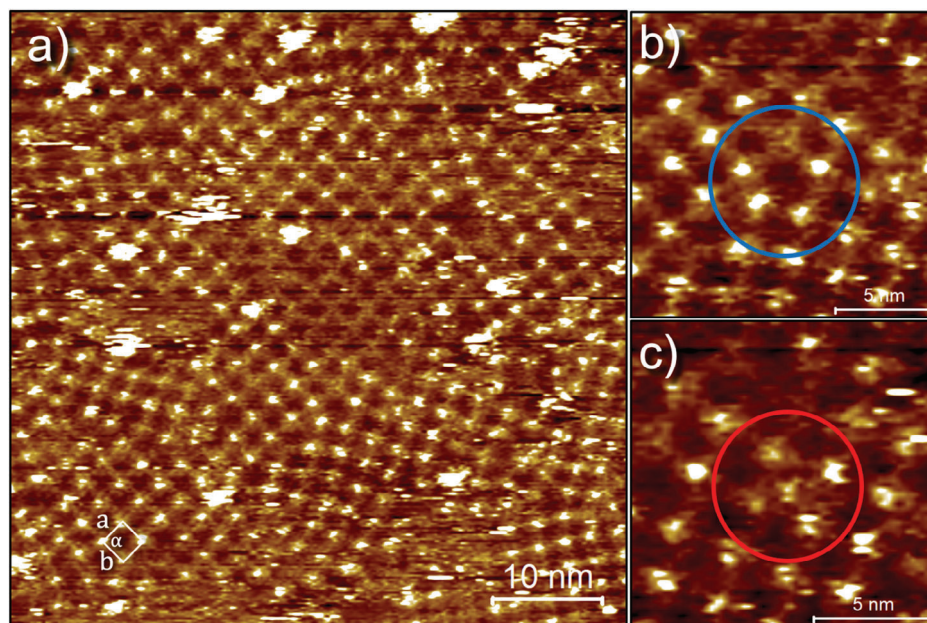
Figure 1. STM images of porphyrin-based s2D-COFs fabricated at room temperature via the seeding approach at the HOPG/HA interface. a) Large-scale STM image of the Fe-porphyrin-based s2D-COF (Fe-s2D-COF). The Fe-containing porphyrins appear bright. Dark patches, just as those in the center of the image are attributed to free-base porphyrins. A unit cell of the square lattice is indicated. b,c) Close view of typical defects found in the C_4 symmetric s2D-COFs such as b) regular pentagons (marked in blue), and c) auto host-guest units (marked in red). Imaging parameters: $V_{bias} = -0.3$ V, I = 0.08 nA.

compared to their simulated counterparts (see Section S5 in Supporting Information for computational details). **Figures 2** and S7 (Supporting Information) show sub-molecular resolution STM images of the porphyrin-based s2D-COFs. The STM contrast of the porphyrins within a free-base s2D-COF is relatively uniform (Figure 2a). The characteristic 4-lobes arising from the pyrrolic rings and the associated depression at the molecular center can be clearly distinguished (blue squares, Figure 2a). This is in line with the corresponding simulated STM image (Figure 2c, Figure S8, Supporting Information).[33] Very similar STM contrast features were also reported in self-assembled molecular networks of (functionalized) free-base TAPP at the solid/liquid interface,[34,35] or for TAPP incorporated in s2D-COFs in ultra-high vacuum conditions.[33]

In the metal-containing s2D-COFs, the porphyrin units within the framework display a distinct and bright protrusion at the center of the monomer unit, indicating the presence of a metal atom (Figure 2b; Figures S7 and S9, Supporting Information).[36–39] STM image simulations were performed by integrating the local density of states (DOS) over a window corresponding to the experimental bias voltage. The center of the monomer, where the Fe metal atom is located, appears bright (Figure 2b,d) as it is in the experimental STM image. The DOS projected onto the metal atom (see Figures S10 and S11, Supporting Information) confirms the presence of metal-atomic states within the energy window, hence contributing to the STM images.[29]

2.3. Single-Layered Porphyrin-based 2D-COF Performance as Heterogeneous Catalyst for CO$_2$RR

The catalytic activity of as-synthesized Fe-TAPP containing s2D-COFs was tested for the electrochemical CO$_2$ reduction reaction.

To do so, after s2D-COF preparation on HOPG, free-base, and Fe-containing samples were rinsed with ethanol to remove any material excess (such as loosely adsorbed monomers as well as the incorporated seed) and dried in air. Considering that the imine linkage within the s2D-COFs is known to be prone to hydrolytic cleavage,[4] the presence of the s2D-COF was further confirmed via STM after such rinsing and drying procedure Figure S12, Supporting Information). AFM data revealed the formation of films with a thickness of ≈0.6 nm (Figure S13 in the Supporting Information).

Cyclic voltammetry (CV) experiments were first carried out in organic media (0.1 M TBAPF$_6$ in acetonitrile, see Section S4 of Supporting Information) using Ar and CO$_2$ atmosphere, respectively. As a proton source, phenol was added to the solution to reach a concentration of 50 mM. To determine the products formed during CO$_2$RR, controlled potential electrolysis (CPE) experiments were carried out. Two consecutive 30-min CPEs were carried out at two different reductive potentials (−1.8 V and −2.1 V versus SCE) employing the functionalized HOPG surface as the working electrode. After identification and quantification of the gaseous products by GC, Faradaic efficiencies (FEs) as well as total and partial current densities were calculated. CPE was also carried out for pristine HOPG without any adsorbed s2D-COF as a control experiment. **Figure 3a** presents the cyclic voltammograms obtained in Ar and CO$_2$ saturated solution for the Fe-s2D-COF. The reduction process under the CO$_2$ atmosphere was lowered by ≈300 mV as compared to the Ar atmosphere, suggesting the existence of a catalytic activity for the electrochemical reduction of CO$_2$. Additionally, there was a clear difference in the current density which rises from ≈1.5 mA cm^{-2} to ≈5 mA cm^{-2} at ≈−2.1 V. In contrast, the difference between the CVs performed in Ar and CO$_2$ when using the metal-free s2D-COF is minimal, which suggests poor
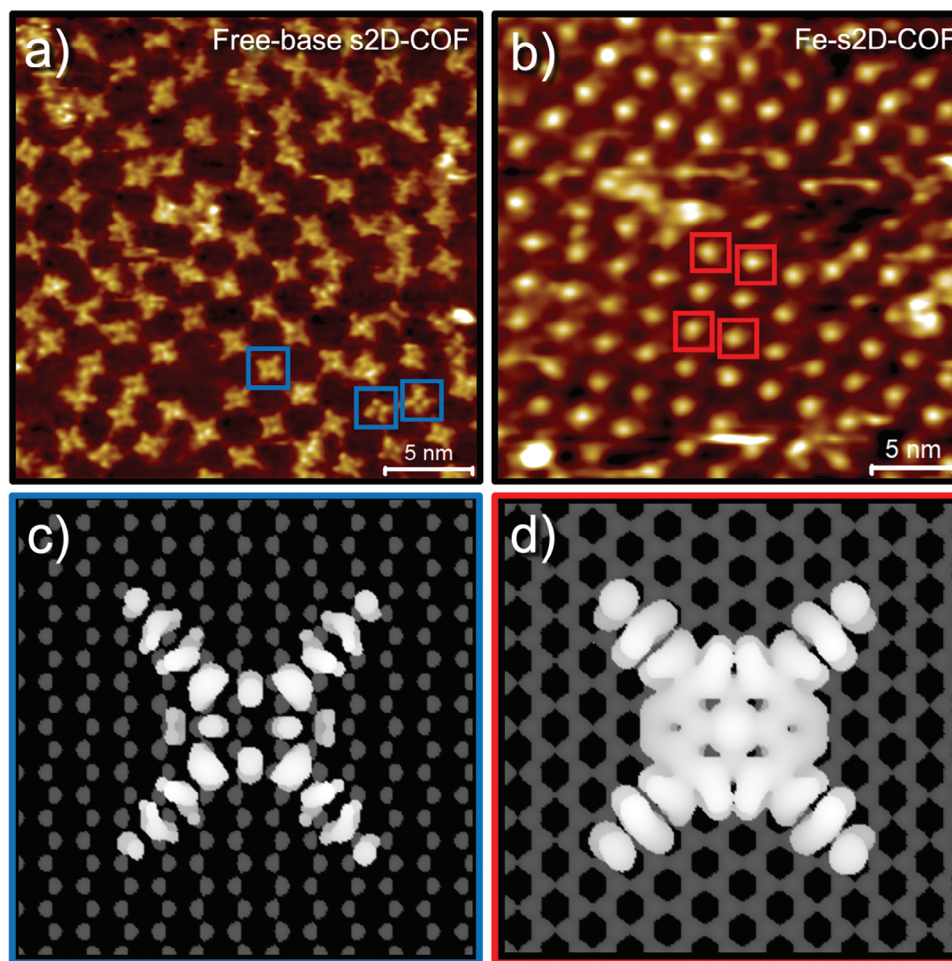
ADVANCED
SCIENCE NEWS
www.advancedsciencenews.com

ADVANCED
ENERGY
MATERIALS
www.advenergymat.de

Figure 2. High-resolution STM images of (a) Free-base (V_{bias} = −0.3 V, I = 0.1 nA) and b) Fe-s2D-COFs (V_{bias} = −1.3 V, I = 0.1 nA) fabricated at the HOPG/HA interface via the seeding method. c,d) Simulated STM images of free-base and Fe-TAPP on graphene, respectively, show the appearance of either a dim or bright center. The experimental bias voltage is used for the STM image simulations.
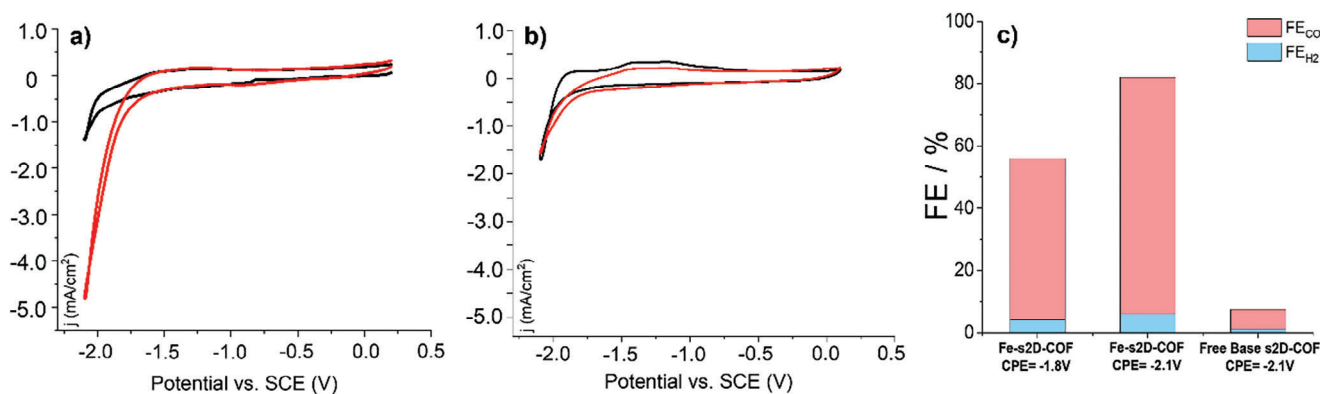

Figure 3. CO_2RR electrochemistry experiments. (a) CV in Ar (black curve) and CO_2 + phenol (red curve) environment of Fe-s2D-COF; (b) CV in Ar (black curve) and CO_2 + phenol (red curve) environment of Fe-TAPP drop cast; and (c) Comparison of the maximum Faradaic efficiencies (FEs) obtained for the CO and H_2 production after 30 min CPE at −1.8 and −2.1 V. CVs scan rate: 100 mV/s. Employed solution in CVs and CPEs: 0.1 M TBAPF$_6$ in acetonitrile. Added acid to CO_2-saturated solution: 50 mM phenol. For CV data of the electrode after the CO_2RR, please see Figure S15 in the Supporting Information.

**ADVANCED
SCIENCE NEWS**

www.advancedsciencenews.com

**ADVANCED
ENERGY
MATERIALS**

www.advenergymat.de

catalytic activity (Figure S14, Supporting Information) of the metal-free s2D-COF. Furthermore, to unambiguously prove that the observed enhanced catalytic activity arises from the Fe centers located within the Fe-s2D-COF adlayer, electrochemical experiments were also carried out for Fe-TAPP monomer drop casted on the surface, even though they do not form a self-assembled network, as described above. Results obtained after the rinsing procedure (Figure 3b) indicate the absence of a catalytic wave when the CV is carried out in a CO_2 environment. It is most likely that the Fe-TAPP monomers were removed from the surface during the rinsing procedure, as they are loosely bound to the surface. This is in contrast to the case where they are incorporated into the more stable and covalently bonded Fe-s2D-COF network (Figure 3a).

Quantitative GC, as well as GC-MS analysis carried out after the CPE experiments indicated that CO and hydrogen (H_2) were the only products of the CO_2 electroreduction for the studied systems and no liquid product was obtained. To confirm the source of carbon in CO production, a CPE using a $^{13}CO_2$ atmosphere was carried out (see Section S4 in Supporting Information) Figure S16 (Supporting Information) shows a GC-MS spectrum obtained after 15 and 30 min electrolysis using Fe-s2D-COF under a $^{13}CO_2$ atmosphere. The peak at m/z = 29 corresponding to ^{13}CO, confirms that the CO produced in the electrolysis process is indeed due to the successful electroreduction of CO_2.

The comparison of calculated FEs for the case of Fe- and free-base-containing s2D-COFs is presented in Figure 3c. Low FEs for the production of CO and H_2 for CPEs performed at −2.1 V versus SCE are observed when employing free-base s2D-COF as catalyst. Also, control electrolysis using the pristine HOPG did not yield any CO_2 reduction product in the investigated conditions. In contrast, Fe-s2D-COF presented much better FEs for the production of CO. In particular, Fe-2D-COF showed 56% FE for CO production with an average partial current density of 1.5 mA cm^{-2} when carrying out the CPE at −1.8 V versus SCE (corresponding to an overpotential $\eta = 839$ mV, see Section S4 in Supporting Information). Conducting a CPE at a lower potential (−2.1 V versus SCE, $\eta = 1139$ mV), (see CV in Figure 3a) showed a higher efficiency and selectivity for the reduction of CO_2 to CO. As presented in Figure 3c, 82% and 6% FE for the formation of CO (93% selectivity) and H_2, respectively, as well as an average partial CO current density of 5.1 mA cm^{-2} (with a maximum of ≈7 mA cm^{-2}, Figure S17, Supporting Information) was obtained. These current densities are higher in comparison with those reported by Kubiak and coworkers (0.5 mA cm^{-2}) obtained under similar conditions, namely CPE at −2.2 V versus Ag/AgCl in acetonitrile, using thin layers of Fe-TAPPCl-based 2D-COFs fabricated on carbon cloth.[9] This difference in current densities suggests that thicker layers, so with more catalyst, may not present better performances than thinner ones or even single-layers of well-defined frameworks with a higher effective surface area of the catalytically active material. A possible explanation for these differences lies in the fact that single or few-layered ordered well-defined frameworks are expected to promote gas diffusion as well as charge transport, which positively affect the electrochemical CO_2RR performances. Additionally, it is possible that for thicker layers, only a few active sites are indeed available for binding with CO_2 which may hinder the overall efficiency as demonstrated earlier for Co-containing 2D-COFs.[8] However, in their study, Kubiak and coworkers[9] and Lin et. al.[8] carried out longer CPEs (3 and 24 h respectively) facilitated by the implementation of carbon cloth and glassy carbon as substrates, in comparison to our short 30 min CPEs on HOPG. The main difference between these substrates lies in the simplicity of their SPM characterization and stability under operando conditions. Therefore, the substrate choice involves a trade-off between the ease of on-surface nanoscale control/characterization and its long-term functionality in targeted applications.

3. Conclusion

We have presented a straightforward method for the room-temperature fabrication of single-layered porphyrin-based imine-linked 2D-COFs for their application in catalyzing electrochemical CO_2 reduction. Our strategy to foster the on-surface fabrication of s2D-COFs is based on the deposition of a COF seed on the HOPG surface, after the addition of a premixed monomer solution, all at ambient pressure and room temperature. STM measurements at the HOPG/liquid interface, combined with STM image simulations, revealed the composition of the s2D-COFs.

The Fe-containing single-layered 2D-COF on graphite was used as electrode for the CO_2 reduction reaction in organic media. Moderate-to-high Faradaic efficiencies as well as current densities along with high selectivity for the reduction of CO_2 to CO, were obtained for short electrolysis performed with the Fe-containing s2D-COF. Our catalysis results present higher performances than similar 2D-COF films with much thicker films. This result shows that single or few-layered systems may overcome thicker films which present much higher catalyst loadings.

Our study indicates that HOPG is a suitable substrate for the on-surface growth of single-layered 2D-COFs, their characterization with (sub)molecular resolution microscopy techniques as well as the extraction of structure-property relationships in proof-of-concept CO_2 reduction catalysis studies. Furthermore, the seeding method could be adaptable for larger surface areas and even other on-surface chemistries as well as well as implemented in other carbon-based (graphene/Cu) or non-carbon-based (Au) substrates.

Supporting Information

Supporting Information is available from the Wiley Online Library or from the author.

Acknowledgements

**ADVANCED
SCIENCE NEWS**

www.advancedsciencenews.com

**ADVANCED
ENERGY
MATERIALS**

www.advenergymat.de

Conflict of Interest

The authors declare no conflict of interest.

Data Availability Statement

The data that support the findings of this study are available from the corresponding author upon reasonable request.

Keywords

[1] C. Costentin, M. Robert, J. M. Savéant, *Chem. Soc. Rev.* **2013**, *42*, 2423.
[2] J. Bonin, A. Maurin, M. Robert, *Coord. Chem. Rev.* **2017**, *334*, 184.
[3] Z. Liang, H. Y. Wang, H. Zheng, W. Zhang, R. Cao, *Chem. Soc. Rev.* **2021**, *50*, 2540.
[4] K. Geng, T. He, R. Liu, S. Dalapati, K. T. Tan, Z. Li, S. Tao, Y. Gong, Q. Jiang, D. Jiang, *Chem. Rev.* **2020**, *120*, 8814.
[5] J. Guo, D. Jiang, *ACS Cent. Sci.* **2020**, *6*, 869.
[6] C. S. Diercks, Y. Liu, K. E. Cordova, O. M. Yaghi, *Nat. Mater.* **2018**, *17*, 301.
[7] D. H. Nam, P. De Luna, A. Rosas-Hernández, A. Thevenon, F. Li, T. Agapie, J. C. Peters, O. Shekhah, M. Eddaoudi, E. H. Sargent, *Nat. Mater.* **2020**, *19*, 266.
[8] S. Lin, C. S. Diercks, Y. B. Zhang, N. Kornienko, E. M. Nichols, Y. Zhao, A. R. Paris, D. Kim, P. Yang, O. M. Yaghi, C. J. Chang, *Science* **2015**, *349*, 1208.
[9] P. L. Cheung, S. K. Lee, C. P. Kubiak, *Chem. Mater.* **2019**, *31*, 1908.
[10] T. H. Phan, K. Banjac, F. P. Cometto, F. Dattila, R. García-Muelas, S. J. Raaijman, C. Ye, M. T. M. Koper, N. López, M. Lingenfelder, *Nano Lett.* **2021**, *21*, 2059.
[11] Y. Liang, K. Banjac, K. Martin, N. Zigon, S. Lee, N. Vanthuyne, F. A. Garcés-Pineda, J. R. Galán-Mascarós, X. Hu, N. Avarvari, M. Lingenfelder, *Nat. Commun.* **2022**, *13*, 3356.
[12] B. Wurster, D. Grumelli, D. Hötger, R. Gutzler, K. Kern, *J. Am. Chem. Soc.* **2016**, *138*, 3623.
[13] G. Zhan, Z. F. Cai, K. Strutyński, L. Yu, N. Herrmann, M. Martínez-Abadía, M. Melle-Franco, A. Mateo-Alonso, S. D. Feyter, *Nature* **2022**, *603*, 835.
[14] R. Tanoue, R. Higuchi, N. Enoki, Y. Miyasato, S. Uemura, N. Kimizuka, A. Z. Stieg, J. K. Gimzewski, M. Kunitake, *ACS Nano* **2011**, *5*, 3923.
[15] Y. Yu, J. Lin, Y. Wang, Q. Zeng, S. Lei, *Chem. Commun.* **2016**, *52*, 6609.
[16] L. Xu, X. Zhou, Y. Yu, W. Q. Tian, J. Ma, S. Lei, *ACS Nano* **2013**, *7*, 8066.
[17] Y. Hu, N. Goodeal, Y. Chen, A. M. Ganose, R. G. Palgrave, H. Bronstein, M. O. Blunt, *Chem. Commun.* **2016**, *52*, 9941.
[18] X. H. Liu, C. Z. Guan, S. Y. Ding, W. Wang, H. J. Yan, D. Wang, L. J. Wan, *J. Am. Chem. Soc.* **2013**, *135*, 10470.
[19] S. Tan, S. R. Wang, Q. Zeng, Y. Liu, *ACS Appl. Mater. Interfaces* **2022**, *14*, 40173.
[20] N. Bilbao, Y. Yu, L. Verstraete, J. Lin, S. Lei, S. D. Feyter, *Chem. Commun.* **2018**, *54*, 9905.
[21] V. Mishra, V. K. Yadav, J. K. Singh, T. G. Gopakumar, *Chem.- Asian J.* **2019**, *14*, 4645.
[22] X. H. Liu, Y. P. Mo, J. Y. Yue, Q. N. Zheng, H. J. Yan, D. Wang, L. J. Wan, *Small* **2014**, *10*, 4934.
[23] W. Dong, L. Wang, H. Ding, L. Zhao, D. Wang, C. Wang, L. J. Wan, *Langmuir* **2015**, *31*, 11755.
[24] N. Herrmann, C. Martin, S. Eyley, Y. Li, N. Bilbao, V. Rubio-Giménez, M. V. der Auweraer, W. Thielemans, L. Chen, K. S. Mali, S. D. Feyter, *Chem. Commun.* **2023**, *59*, 9211.
[25] Y. P. Mo, X. H. Liu, D. Wang, *ACS Nano* **2017**, *11*, 11694.
[26] D. Cui, D. F. Perepichka, J. M. MacLeod, F. Rosei, *Chem. Soc. Rev.* **2020**, *49*, 2020.
[27] C. Costentin, M. Robert, J. M. Savéant, *Acc. Chem. Res.* **2015**, *48*, 2996.
[28] S. Gu, A. N. Marianov, T. Lu, J. Zhong, *Chem. Eng. J.* **2023**, *470*, 144249.
[29] J. Herritsch, S. R. Kachel, Q. Fan, M. Hutter, L. J. Heuplick, F. Münster, J. M. Gottfried, *Nanoscale* **2021**, *13*, 13241.
[30] X. Deng, D. Alfonso, T. D. Nguyen-Phan, D. R. Kauffman, *ACS Catal.* **2022**, *12*, 5921.
[31] J. F. Dienstmaier, A. M. Gigler, A. J. Goetz, P. Knochel, T. Bein, A. Lyapin, S. Reichlmaier, W. M. Heckl, M. Lackinger, *ACS Nano* **2011**, *5*, 9737.
[32] J. Yang, B. Tu, G. Zhang, P. Liu, K. Hu, J. Wang, Z. Yan, Z. Huang, M. Fang, J. Hou, Q. Fang, X. Qiu, L. Li, Z. Tang, *Nat. Nanotechnol.* **2022**, *17*, 622.
[33] C. Chen, T. Joshi, H. Li, A. D. Chavez, Z. Pedramrazi, P. N. Liu, H. Li, W. R. Dichtel, J. L. Bredas, M. F. Crommie, *ACS Nano* **2018**, *12*, 385.
[34] M. O. Blunt, Y. Hu, C. W. Toft, A. G. Slater, W. Lewis, N. R. Champness, *J. Phys. Chem. C* **2018**, *122*, 26070.
[35] A. G. Slater, Y. Hu, L. Yang, S. P. Argent, W. Lewis, M. O. Blunt, N. R. Champness, *Chem. Sci.* **2015**, *6*, 1562.
[36] A. Bhattarai, K. Marchbanks-Owens, U. Mazur, K. W. Hipps, *J. Phys. Chem. C* **2016**, *120*, 18140.
[37] X. Lu, K. W. Hipps, *J. Phys. Chem. B* **1997**, *101*, 5391.
[38] X. Lu, K. W. Hipps, X. D. Wang, U. Mazur, *J. Am. Chem. Soc.* **1996**, *118*, 7197.
[39] M. Bouatou, R. Harsh, F. Joucken, C. Chacon, V. Repain, A. Bellec, Y. Girard, S. Rousset, R. Sporken, F. Gao, M. Brandbyge, Y. J. Dappe, C. Barreteau, A. Smogunov, J. Lagoute, *J. Phys. Chem. Lett.* **2020**, *11*, 9329.